Multiple Actin Binding Domains of Ena/VASP Proteins Determine Actin Network Stiffening

Brian S. Gentry[1], Stef van der Meulen[1], Philippe Noguera[2], Julie Plastino[2] and Gijsje H. Koenderink[1*]

[1]*Biological Soft Matter Group, FOM Institute AMOLF, Science Park 104, 1098 XG Amsterdam, The Netherlands*

[2]*Institut Curie, Centre National de la Recherche Scientifique, Université Pierre et Marie Curie, Paris F-75248, France*

**Corresponding author*. Tel.: +31(20) 754-7100; Fax: +31(20)-754-7290; E-mail: g.koenderink@amolf.nl

Abstract

Vasodilator-stimulated phosphoprotein (Ena/VASP) is an actin binding protein, important for actin dynamics in motile cells and developing organisms. Though VASP's main activity is the promotion of barbed end growth, it has an F-actin binding site and can form tetramers, and so could additionally play a role in actin crosslinking and bundling in the cell. To test this activity, we perform rheology of reconstituted actin networks in the presence of wild type VASP or mutants lacking the ability to tetramerize or to bind G-actin and/or F-actin. We show that increasing amounts of wild type VASP increase network stiffness up to a certain point, beyond which stiffness actually decreases with increasing VASP concentration. The maximum stiffness is 10-fold higher than for pure actin networks. Confocal microscopy shows that VASP forms clustered actin filament bundles, explaining the reduction in network elasticity at high VASP concentration. Removal of the tetramerization site results in

significantly reduced bundling and bundle clustering, indicating that VASP's flexible tetrameric structure causes clustering. Removing either the F-actin or the G-actin binding site diminishes VASP's effect on elasticity, but does not eliminate it. Mutating the F-actin and G-actin binding site together, or mutating the F-actin binding site and saturating the G-actin binding site with monomeric actin, eliminates VASP's ability to increase network stiffness. We propose that, in the cell, VASP crosslinking confers only moderate increases in linear network elasticity, and unlike other crosslinkers, VASP's network stiffening activity may be tuned by the local concentration of monomeric actin.

Keywords

cell mechanics; rheology; cytoskeleton; viscoelasticity; crosslinking

Introduction

Ena/VASP is a family of proteins found in vertebrates, invertebrates and *Dictyostelium* whose members play important roles in many actin remodelling processes in cells and developing organisms (Reinhard et al. 2001; Krause et al. 2002). Examples include fibroblast rigidity, adhesion and migration(Bear et al. 2000; Galler et al. 2006) formation of endothelial junctions in mice (Furman et al. 2007); development of the human cerebral cortex (Yaba et al 2011); formation of filopodia in fibroblasts, *Dictyostelium* and neuronal growth cones; neurite growth and neuronal guidance (Applewhite et al. 2007; Schirenbeck et al. 2006; Lebrand et al. 2004; Kwiatkowski et al. 2007); and movement of *Listeria monocytogenes* (Laurent et al. 1999). *In vitro*, VASP influences actin assembly through binding of actin monomers, filaments and profilin-actin (Walders-Harbeck et al. 2002; Chereau and Dominguez 2006; Hansen et al. 2010); promotes filament elongation (Hansen et al. 2010; Plastino et al. 2004; Breitsprecher et al. 2008); interferes with barbed end capping (Bear et al. 2002; Barzik et al. 2005); bundles filaments (Schirenbeck et al. 2006; Bachmann et al. 1999; Hüttelmaier et al. 1999);

and influences bead motility in reconstituted systems (Plastino et al. 2004; Samarin et al. 2003; Trichet et al. 2007). Moreover, a recent AFM nanoindentation study of actin comet tails grown from VASP-coated beads showed increases in tail stiffness (Suei et al. 2011).

All Ena/VASP proteins share a highly conserved domain structure, with an N-terminal Ena/VASP homology 1 (EVH1) region and a C-terminal Ena/VASP homology 2 (EVH2) region separated by a proline-rich core (Reinhard et al. 2001; Kwiatkowski et al. 2003), as illustrated in Fig. 1a. The EVH1 domain binds to numerous ligands important for cytoskeletal regulation, including the actin binding proteins zyxin, vinculin, and ActA (Reinhard et al. 2001). The EVH2 domain is responsible for interaction with actin and contains a globular G-actin binding site (GAB) and a filamentous F-actin binding site (FAB), both of which can bind F-actin (Hansen et al. 2010). EVH2 also contains a tetramerization motif (TET). Between the EVH1 and EVH2 domains lies a proline-rich region (Poly Pro) adjacent to the GAB site that promotes addition of profilin-actin complexes at filament barbed ends (Ferron et al. 2007). The VASP molecule is long and flexible. While its real dimensions are not known, since a crystal structure of the full-length molecule is lacking, the EVH1 domain alone already has an average end-to-end length of 40 nm (Breitsprecher et al. 2008).

Based on VASP's multiple domain structure, it has been proposed that it can have a complex range of possible interactions with actin monomers, actin filaments and actin binding proteins (Bear and Gertler 2009), as sketched in Fig. 1b. Experiments have indeed demonstrated a number of VASP-actin interactions, including both actin filament end-binding and side-binding modes. It was shown that VASP may regulate the cytoskeleton via actin assembly at filament barbed ends, where it stably binds and promotes elongation through monomer addition. In this capacity it can bind both monomeric actin and profilin-actin complexes through its GAB site, while the FAB site transiently binds to the filament side (Hansen et al. 2010; Breitsprecher et al. 2011; Pasic et al. 2008). The side-binding capacity may be particularly important to insure actin filament stabilization and tethering during elongation when VASP

is confined to a substrate (Schirenbeck et al. 2006; Laurent et al. 1999; Hansen et al. 2010), but it may also help bundle actin filament tips in filopodia (Schirenbeck et al. 2006; Lebrand et al. 2004; Hansen et al. 2010). A more stable side-binding mode in which both GAB and FAB domains bind actin filaments is presumably responsible for the formation of composite filament/bundle networks *in vitro* (Laurent et al. 1999; Breitsprecher et al. 2008; Barzik et al. 2005; Bachmann et al. 1999; Skoble et al. 2001), though there is also evidence that this bundling initiates from interactions at the barbed end (Pasic et al. 2008). It is not known if VASP also crosslinks actin filaments and stiffens *in vitro* networks through side-binding, nor is it clear to what extent these effects are important under cellular conditions.

VASP's different actin binding modes can be modified by free actin monomers which antagonize side binding and promote end binding by occupation of the GAB domain (Hansen et al. 2010). Thus, VASP-actin interactions may be tuned by the participation of different domains in actin binding. Interactions may also be significantly modified by numerous physiologically relevant factors such as buffer ionic strength, VASP and actin concentration, substrate confinement or molecular crowding (Breitsprecher et al. 2008). Because nucleation, tetramerization, and bundling are all interrelated and accounted for by the EVH2 domain found in each of VASP's four flexible arms, VASP-actin interactions may be strongly influenced by the local cytoskeletal environment (Chereau and Dominguez 2006).

Because VASP-actin interactions are complex, it is important to study them in simplified and controlled systems. Elucidating the structural and mechanical properties of filament networks bundled by VASP provides a straightforward way to gain a better understanding of actin-VASP interactions. We examine the microstructure and viscoelastic properties of networks reconstituted from purified actin and VASP in a range of physiologically relevant concentrations. Use of VASP mutants and free actin monomers to study the effects of distinct VASP domains on network mechanics and structure sheds new light on the complexity of VASP-actin interactions.

Materials and methods

Materials

Recombinant murine His-tagged wild type VASP and VASP mutant proteins were prepared as described elsewhere (Barzik et al. 2005; Pasic et al. 2008). Concentrations of all VASP mutants were determined by a Bradford assay and reported values represent the tetramer. Actin was purified according to the method of Pardee and Spudich (Pardee and Spudich 1982), including a gel filtration step on a HiPrep Sephacryl 26/60 column (Åkta), or purchased from Cytoskeleton (sedimentation assays). The actin concentration was quantified by measuring light absorbance at 290 nm using an extinction coefficient of 0.62 ml/mg (Loisel et al. 1999). Alexa 594-labelled G-actin was prepared following the manufacturer's instructions using Alexa Fluor 594 carboxylic acid succinimidyl ester (Invitrogen) at pH 8, followed by dialysis against G Buffer (Tris HCl 2 mM, $CaCl_2$ 0.2 mM, dithiothreitol (DTT) 0.2 mM, pH 8.0) to remove excess dye. Proper function of fluorescently labelled actin at a ratio of 1 labelled to 10 unlabelled monomers was verified by the formation of comet tails in a bead motility assay (Plastino et al. 2004). The average length of fluorescently labelled filaments was 8 μm. For all protein concentration measurements a Nanodrop 2000 spectrophotometer (Thermo Scientific) was used. Latrunculin-actin was prepared using a 5-fold molar excess of latrunculin B (Santa Cruz Biotechnology) and was incubated in G-buffer for 30 min on ice prior to experiments.

Confocal microscopy

Sample chambers were prepared by cleaning glass coverslips and microscope slides by sonication in 50% ethanol, followed by sonication and rinsing with Milli-Q water. Slivers of coverslips were used as spacers to create chambers with a nominal volume of 22 μl. Slides, spacers and coverslips were bonded using optical adhesive (Norland). Chambers were passivated with 0.1 mg/ml kappa-casein for 5 min

and then washed with X-buffer (10 mM Hepes, 0.1 mM KCl, 1 mM $MgCl_2$, and 0.1 mM $CaCl_2$). For VASP-actin samples, first Mg-G-actin (10% fluorescently labelled and 90% unlabelled) was prepared by incubation in a 1 molar equivalent plus 10 μM $MgCl_2$ and 0.2 mM EGTA in G-buffer (2 mM Tris 0.2 mM $CaCl_2$, 0.2 mM DTT pH 8) and incubating on ice for 5 min. VASP proteins were added to Mg-G-actin before polymerization. The final samples contained 10 mM Hepes, pH 7.5, 115 mM KCl, 2.1 mM Mg-ATP, 7 mM DTT, and 150 μM DABCO. These buffer conditions are similar to those used in typical actin comet tail assays (Plastino et al. 2004; Loisel et al. 1999; Wiesner et al. 2003). We verified by confocal microscopy that the Mg^{2+} ions at the concentration used in these studies did not cause bundling in the presence of VASP (Online Resource 1) nor with actin alone (Online Resource 2c). For latrunculin-actin samples, actin was allowed to polymerize for 5 min at room temperature in the presence of VASP before addition of latrunculin-actin. Samples were polymerized at room temperature for 45 min. Fluorescent actin was illuminated with a Melles Griot 543 nm laser and observed using a Nikon Eclipse C1Si confocal head fitted to a Nikon Eclipse Ti inverted microscope using a 40x apochromatic oil objective (1.0 NA). Image stacks in the z-direction were automatically obtained using Nikon EZC1 software with 35 images taken at 1.5 μm intervals. Maximum intensity projections were created using ImageJ and the contrast of each projection was identically enhanced (normalized with 0.4% saturated pixels). For homogeneous filament networks, single plane images were recorded. These images were bandpass filtered between 1 and 40 pixels to remove large wavelength variations in light intensity.

Macroscopic shear rheology and LAOS analysis

Samples were prepared at 35.7 μM actin with a 125 μl sample volume in the same manner as for confocal microscopy. Immediately after mixing, samples were pipetted onto the steel bottom plate of a stress-controlled rheometer (Anton Paar Physica MCR 501, Graz, Austria) set at 20^{o}C. Actin was

polymerized between the bottom plate and a 30 mm diameter steel cone (0.988° angle, 58 µm truncation). Polymerization was monitored by measuring the increase in the elastic and viscous shear modulus with an oscillating shear at a frequency, ω, of 3.1 rad/s and small strain amplitude, γ, of 0.5%. In the linear regime, the ratio of the stress response, $\sigma(\omega)$, to the applied strain equals the complex shear modulus, $G^*(\omega) = G'(\omega) + iG''(\omega)$. The elastic modulus, $G'(\omega)$, represents the in-phase (storage) response, while the viscous modulus, $G''(\omega)$, represents the out-of-phase (loss) response. The frequency dependent moduli of actin-VASP networks were measured by oscillatory tests using γ = 2.0% and ω = 3.1-0.031 rad/s.

Nonlinear shear rheology was performed with the same rheometer and cone-plate geometry using the large amplitude oscillatory shear (LAOS) method. We used this method instead of commonly used prestress and step-stress protocols (Gardel et al. 2006, Broedersz et al. 2008, Semmrich et al. 2008), because we observed substantial creep of actin-VASP networks when a steady shear (even within the linear regime) was applied. The rheometer provides stress and strain data averaged over 3 cycles. Since the raw LAOS data at large strain showed clear deviations from a sinusoidal (linear) stress response, we analyzed nonlinearities in the elastic response using a previously described method (Ewoldt et al. 2008). Nonlinearities in the elasticity are well described by the ratio of the first and third coefficients of Chebychev polynomials of the first kind, which are related to the Fourier transform of the stress signal. A coefficient ratio of e_3/e_1 is zero in the linear regime, while $e_3/e_1 > 0$ indicates intra-cycle strain-stiffening, i.e. strain-stiffening within an oscillation cycle. This parameter suffers less from noise than other elasticity parameters, and provides a sensitive measure of deviations from linear elasticity (Ewoldt et al. 2008).

Co-sedimentation assays

G-actin (purchased from Cytoskeleton) was charged with Mg^{2+} by incubation in a 1 molar equivalent plus 10 µM $MgCl_2$ and 0.2 mM EGTA in G-buffer (2 mM Tris 0.2 mM $CaCl_2$, 0.2 mM DTT pH 8) on ice for 5 min. Actin was then diluted to 12 µM in X-buffer (10 mM HEPES pH 7.5, 0.1 M KCl, 1 mM $MgCl_2$, 0.1 mM $CaCl_2$), supplemented with 1.8 mM ATP, 3.6 mM $MgCl_2$, 130 µM DABCO, 6 mM DTT and the appropriate amount of VASP or VASP mutants in VASP buffer (20mM imidazole, pH 7.0, 200mM KCl, 1mM EGTA, 2mM $MgCl_2$ and 1mM DTT). The final pH was 7.5 and the salt concentration was 110 mM KCl. The reactions were incubated at room temperature for 1 hour and then centrifuged at 12,000 x g for one hour at 4°C to pellet bundles. Supernatants and pellets were separated, denatured in tris-glycine sample buffer, and loaded on 10% polyacrylamide SDS-page gels.

Results

VASP increases the elastic modulus of F-actin networks

We determined whether VASP affects the elastic modulus of actin networks since VASP is rich in specific structures in the cell that are known to sense mechanical cues, such as lamellipodia and filopodia. To this end, rheological measurements were performed on samples with a constant actin concentration (35.7 µM) and crosslink density (VASP:actin ratio) varying from $R = 0.001$ to 0.1. All samples behave as weak viscoelastic solids regardless of VASP concentration, with the elastic modulus G' displaying only a weak frequency dependence (Fig. 2a, left). The loss tangent, $\tan \delta = G''/G'$, calculated at each value of R, shows an elastic modulus only slightly larger than the viscous modulus (Fig. 2a, right), also consistent with weak solid-like behaviour. Figure 2b shows the plateau modulus G_0 (determined at $\omega = 1.15$ rad/s) for increasing VASP:actin molar ratios R. G_0 was 0.40 Pa for actin networks polymerized in the absence of VASP (solid line in Fig. 2b). At low VASP:actin molar ratios

(R = 0.001), G_0 was only slightly higher than F-actin alone (black squares in Fig. 2b). This suggests that there is little crosslinking effect due to VASP in this regime. As R increases, the plateau modulus also increases, but only for values up to R = 0.006. Beginning at R = 0.0125, G_0 decreases with increasing VASP concentration, finally returning to values close to those at low R. This rheological profile differs significantly from that of networks crosslinked by certain other actin binding proteins that are known to crosslink and bundle F-actin, where the elastic modulus steadily increases with increasing crosslinker concentration. The maximum increase in network stiffness observed with VASP is comparable to stiffness increases seen with filamin (Schmoller et al. 2009; Kasza et al. 2009), but an order of magnitude less than that seen for α-actinin, scruin and fascin (Tseng and Wirtz 2001, Tempel et al. 1996; Gardel et al. 2004; Lieleg et al. 2007).

To test the origin of the decrease in linear network elasticity at high VASP to actin molar ratios, we observed the microstructure of VASP-actin networks via confocal imaging. In the absence of VASP, actin networks polymerized at 35.7 μM (1.5 mg/ml) are homogeneous and isotropic (Online Resource 2). When VASP is added, bundles start to appear at a very low threshold of the VASP:actin molar ratio, R = 0.001. As VASP is increased from R = 0.001 to R = 0.006, the network organization changes from composite structures of short straight or curved bundles interspersed in dense filamentous networks to longer, thicker, and more strongly curved fibers (Fig. 2b, top). In addition, large aggregates of intertwined, laterally associated bundles begin to form within these composite bundle/filament networks. This increase in the extent of VASP-mediated bundling as seen by confocal microscopy correlates well with the increase in G_0 measured with rheology (see Fig. 2b, lower). The largest value of G_0 occurs at R = 0.006. At this R value, confocal images show longer, thicker and more strongly curved bundles as compared to lower VASP:actin molar ratios (Fig. 2b, top). The decrease in G_0 observed when the VASP concentration is raised further corresponds to the regime where large bundle aggregates become predominant in the sample. The plateau modulus decreases still further as more

bundles become incorporated into the aggregates at higher R values. At the highest molar ratios, the actin filaments are in very large aggregates of tangled bundles that appear separate (Fig. 2b, top R = 0.1). Overall this profile indicates that despite significant bundling, VASP produces only weakly viscoelastic gels because the composite filament/bundle networks are not interconnected in cohesive, spanning structures that confer a macroscopic stiffness increase. This interpretation is supported by the weak viscoelastic behaviour shown by all samples (Fig. 2b).

In order to further compare VASP's effect on the elastic behaviour of F-actin networks to that of other crosslinkers, nonlinear rheology was performed at R = 0.006 corresponding to the maximum increase in the linear elastic modulus. We used the large amplitude oscillatory shear (LAOS) method, in which filament networks are subjected to strain oscillations at a constant frequency (here 0.1 Hz) with increasing strain amplitude γ_0. Figure 3 (inset) shows Lissajous figures generated by plotting the stress $\sigma(t)$ as a function of the applied strain $\gamma(t)$ for three strains – 2.0% (innermost curve), 22.2% (middle curve), and 73.9% (outermost curve). The shape of these curves provides a signature of nonlinear response. At small strains the response is linear (inner curve), as evident from the elliptical shape of the Lissajous curve. At higher strains the curve deviates from an ellipse with a small upturn at maximum strain (middle curve) indicating moderate intra-cycle stiffening. Finally, the trajectory becomes distorted as the network approaches mechanical failure and rupture (outer curve). The ratio of the first and third Chebychev coefficients plotted against γ_0 (Fig. 3, squares) confirms that F-actin networks containing VASP produced only moderate strain stiffening at high strains. Furthermore, the strain-stiffening behaviour of VASP-mediated actin networks was not significantly different from that of F-actin alone (Fig. 3, circles). This supports evidence from linear rheology that VASP does not strongly crosslink F-actin networks.

The effect of VASP on linear network elasticity is due to a combination of VASP's actin binding domains and tetrameric structure

To elucidate the role of VASP's multiple actin binding domains in increasing network stiffness via F-actin crosslinking/bundling, we generated VASP mutants in which the GAB and FAB sites were separately rendered non-functional, either by mutation (mGAB) or deletion (ΔFAB), as well as a mutant lacking both sites (ΔFABGAB). Rheological measurements were performed on VASP wild type and mutants at $R = 0.025$ and $c = 35.7$ μM, conditions where wild type VASP is close to its optimum in terms of stiffness increase. As expected, ΔFAB produces a smaller increase in network stiffness than wild type VASP. Surprisingly, however, ΔFAB is still able to increase stiffness over the background level of pure F-actin, indicating that there must be other sites on the VASP molecule capable of binding F-actin (Fig. 4b). The G-actin binding (GAB) site seems to be a likely candidate, since the mGAB mutation greatly reduces VASP's ability to increase network stiffness compared to wild type VASP. Removal of both actin-binding sites (ΔFABGAB) indeed reduces the plateau modulus to that of F-actin only. As an alternative test of F-actin binding by the GAB site, we treated the ΔFAB mutant with 4 μM of latrunculin-actin, which provides a pool of unpolymerizable actin monomers. This treatment reduced the plateau modulus to that of F-actin only (Fig. 4a), confirming that the GAB site contributes to the F-actin crosslinking/bundling activity of VASP and can maintain a certain level of crosslinking in the absence of the F-actin binding site. However, this crosslinking activity occurs only when the GAB domain is not complexed with monomeric actin.

We can also observe this effect by confocal fluorescence microscopy and sedimentation assays. The ΔFAB mutant displays bundling activity, presumably via the GAB site (Online Resource 3), since when both sites are removed (ΔFABGAB) only small actin punctae are observed within the actin network (Online Resource 4). Additionally, when the ΔFAB mutant is treated with 4 μM of latrunculin-actin,

bundles are no longer formed (Fig. 4b). Consistent with the rheology measurements, these results indicate that the GAB site causes bundling even in the absence of the F-actin binding domain, but only when it is not bound with monomeric actin. These results were further confirmed by a low-speed sedimentation assay at 11.9 μM actin (Fig. 4c). In this assay, only filamentous actin that is incorporated into bundles or aggregates will be pelleted, while free filaments will remain in the supernatant. At R = 0.05, (Fig. 4c**)**, only the ΔFABGAB mutant displays almost no pelleted actin, while mGAB and ΔFAB show a considerable amount, although less than wild type. This confirms the observation made by confocal microscopy that the GAB and FAB sites both appear to participate in F-actin bundling.

To determine the contribution of VASP's tetrameric structure to F-actin bundling, networks containing a VASP mutant lacking the tetramerization (ΔTET) site were observed using confocal microscopy. Bundling was dramatically reduced in all samples, and very few aggregates were observed, even at high R values. Figure 4d illustrates the contrast in bundling between VASP wild type and the dTET mutant at c = 35.7 μM and R = 0.1. Thus, the tetrameric structure of VASP plays a crucial role in producing large bundles and aggregates thereof.

VASP-mediated bundling and aggregate formation also depend upon actin concentration

Confocal images of VASP-mediated F-actin bundling also show that the onset actin:VASP molar ratio R for bundling depends on F-actin concentration. In the absence of VASP, networks are homogeneous and isotropic for all concentrations tested (Online Resource 2). Figure 5 shows the transition from homogeneous filament networks to networks containing bundles for samples with VASP at three different actin concentrations. As the actin concentration is lowered, the actin:VASP molar ratio where bundles first appear goes up, from 0.001 at 35.7 μM (1.5 mg/ml) actin to 0.003 at 11.9 μM (0.5 mg/ml) (Fig. 5, compare left-hand and middle columns). At an R value of 0.05, all actin

concentrations tested showed primarily large aggregated bundle structures, but these aggregates were largest at the highest actin concentration (Fig. 5, right-hand column).

Discussion

Our rheological measurements of VASP-mediated F-actin bundling in solution show that, unlike crosslinking/bundling proteins such as fascin, VASP confers only modest increases in linear network elastic modulus and does not substantially modify the nonlinear response even at high VASP concentrations. This is consistent with a recent study using atomic force microscopy to probe the elasticity of actin comet tails grown from microspheres. The presence of low concentrations of VASP in the solution had no detectable effect upon the elastic modulus of the comets (Suei et al. 2011).

The stiffness dependence on VASP:actin molar ratio is directly reflected by changes observed in bundle network morphology. Confocal images allow observation of the overall appearance of large sample areas and help to explain the macroscopic elastic behaviour of the networks. The maximum increase in stiffness occurs in networks of long entangled bundles at intermediate molar ratios, whereas the drop in the plateau modulus with decreasing R corresponds with the formation of large aggregates (Fig. 5). These observations are consistent with finite element simulations, which predict that clustering in composite bundle/filament networks drastically reduces stiffness as more material becomes incorporated in localized, heterogeneous structures (Lieleg et al. 2009).

Bundle cluster networks have also been observed with α-actinin and filamin at actin concentrations of 24 μM. These actin-binding proteins, like VASP, are long and flexible, whereas shorter and stiffer molecules such as fascin and scruin produce composite filament/bundle networks or even pure bundled phases without clusters (Schmoller et al. 2009; Lieleg et al. 2007; Lieleg et al. 2009; Shin et al. 2004; Lieleg et al. 2010). Previous work already showed that bundle cluster networks are

associated with a weaker mechanical response as compared to the large increases in G_0 observed with fascin and scruin (Lieleg et al. 2010). However, drastic decreases in elastic response due to clustering have not been previously observed. Filamin, like VASP, produces very large clusters at higher crosslink concentrations, but shows a modest overall *increase* in linear elasticity (Schmoller et al. 2009; Kasza et al. 2009); α-actinin shows a weaker plateau modulus increase in the bundle cluster regime compared to the mixed bundle phase (Lieleg et al. 2009). Neither α-actinin nor filamin, however, show an actual decrease in elasticity due to clustering. VASP-mediated networks display a marked decrease in the elastic modulus at the onset of bundle clustering, and the modulus continues to decrease with increasing VASP concentration. The elastic response eventually returns to a value similar to that induced by low VASP concentrations. Overall, this suggests that, despite bundle cluster formation, α-actinin and filamin play a stronger crosslinking role in F-actin networks than does VASP.This conclusion is supported by the moderate strain-stiffening behaviour of VASP-actin networks at high strains, which is indistinguishable from that of pure F-actin solutions. This behaviour is in contrast to the marked strain-stiffening observed with other crosslinking and bundling proteins such as α-actinin, filamin, heavy meromyosin and fascin (Xu et al. 2000, Gardel et al. 2006, Kasza et al. 2006, Schmoller et al. 2009, Tharmann et al. 2007, Lieleg et al. 2006).

In the absence of free actin monomers, we show that both the FAB and GAB domains of VASP individually increase network stiffness above that of pure F-actin, though both produce a smaller effect than the wild type. This result is confirmed by confocal microscopy and sedimentation assays that show that either domain is sufficient for some bundle formation, but only at high VASP:actin molar ratios (Fig. 4). While it has previously been shown that the FAB domain is sufficient to produce filament bundling, we also observed bundling in the mutant lacking the FAB site (Online Resource 3). We even observed loose bundling by the mutant lacking both FAB and GAB sites, though only at the highest actin concentrations and highest VASP:actin molar ratios (Online Resource 4). This surprising finding

is actually consistent with prior observations that both *Dictyostelium* and murine VASP mutants lacking the GAB and FAB domains were able to capture filaments on surfaces, suggesting an additional F-actin binding site on VASP's C-terminal region (Breitsprecher et al. 2008; Pasic et al. 2008). Finally, we show by confocal microscopy that the tetrameric structure of VASP is necessary to produce a significant degree of bundling and aggregation, even when both G- and F-actin binding domains are present (Fig. 4d).

Although the GAB domain participates in F-actin bundling in our assay, it may not when it is in contact with the high concentrations of G-actin that are present in the cell, which we mimicked in this study with sequestered latrunculin-actin. Indeed, free actin monomers reduce or eliminate bundling with VASPΔFAB at low actin concentrations. Presumably, this mutant binds actin filaments via its GAB domain, which is competitively displaced from F-actin in the presence of monomeric actin. These results echo, in part, recent findings using single molecule detection of VASP on actin filaments by total internal reflection fluorescence (TIRF) microscopy, where it was observed that mutating the GAB domain or saturating this site with monomeric actin compromises filament binding by VASP, although deletion of the FAB domain in this same study completely abrogated VASP's ability to interact with F-actin (Hansen et al. 2010). Filament bundling by VASP thus appears very sensitive to the free actin monomer concentration, the ratio between the amount of F-actin and VASP, and also to the F-actin concentration, which changes the thresholds for the onset of bundling and the predominance of aggregates within the networks.

We propose that the observed F-actin bundling behaviour of wild type and mutant VASP results from the structural arrangement of multiple actin binding sites on flexible VASP tetramers. This proposal is in line with prior models based on observations of VASP interaction with actin monomers and filaments (Bear and Gertler 2009) (Fig. 1b). VASP's flexible tetrameric structure can explain the dependence of bundle morphology on both *c* and *R*, as more VASP or more actin filaments allow

connections between multiple filaments and bundles in various alignments and configurations. The flexible tetrameric structure also explains VASP's ability to bundle at very low VASP:actin molar ratios and to form aggregates at high molar ratios, because each VASP can bind up to four actin filaments. In order to more thoroughly understand the formation of aggregates at higher *R* values, details of individual bundle morphology at high magnification must be considered. Previous electron microscopy observations of VASP-mediated F-actin bundles in buffers of similar ionic strength show loosely packed bundles with many single filaments emanating at multiple angles, and displaying no long range internal order (Laurent et al. 1999; Barzik et al. 2005). This suggests that as the VASP:actin molar ratio is increased, the number of VASP-mediated interactions between filaments emanating from different bundles will also increase. Transmission electron microscopy and analytical centrifugation have shown that the VASP molecule is very flexible (Breitsprecher et al. 2008), so connections between bundles will have little bending energy cost, resulting in numerous lateral associations between bundles that are often strongly curved (Fig. 5) Because bundles tend to be quite long at the highest *R* values (30 μm or more), more bundle-bundle interactions will occur along the long axis of the fibers, producing large aggregates within the composite networks.

The sensitive dependence of VASP-mediated bundling in solution on actin and VASP concentrations that we demonstrate here may be particularly relevant to cells, where F-actin concentrations have been estimated to be in the range of 12-300 μM (Pollard et al. 2000). In some localized regions, such as the lamellipodia of migrating cells, F-actin levels can reach values as high as 500 μM (Koestler et al. 2009), and actin comet tails have been estimated to be in the millimolar range in F-actin (Wiesner et al. 2003). In addition, intracellular profilin-actin concentrations can also be quite high (5-40 μM), possibly providing a means by which bundling interactions can be tuned (Ferron et al. 2007). We propose that VASP does not function as a bona fide crosslinking protein conferring global increases in network stiffness, but rather bundles near the leading edge or in filopodia where local F-

actin and VASP concentrations are high. Monomer depletion in rapidly expanding zones may equally allow for transient increases in VASP bundling activity.

Acknowledgements

This work was funded by a Human Frontier Science Program Young Investigator Grant No. RGY0085/2009-C (to J.P. and G.H.K.) and is part of the research program of the 'Stichting voor Fundamenteel Onderzoek der Materie (FOM)', which is financially supported by the 'Nederlandse Organisatie voor Wetenschappelijk Onderzoek (NWO)'. We are grateful to Marjolein Kuit-Vinkenoog (AMOLF) and John Manzi (Institut Curie) for invaluable help with VASP purifications. We thank Dorothy Schafer for the VASP constructs and useful discussions, and Roberto Dominguez, Marjolein Kuit-Vinkenoog, Sandy Suei, Laurent Kreplak, José Alvarado, and Björn Stuhrmann for useful discussion. We thank Baldomero Alonso Latorre for help with LAOS analysis.

References

Applewhite DA, Barzik M, Kojima S, Svitkina TM, Gertler FB, Borisy GG (2007) Ena/VASP Proteins Have an Anti-Capping Independent Function in Filopodia Formation. Mol Biol Cell 18:2579–2591

Bachmann C, Fischer L, Walter U, Reinhard M (1999) The EVH2 Domain of the Vasodilator-stimulated Phosphoprotein Mediates Tetramerization, F-actin Binding, and Actin Bundle Formation. J Biol Chem 274:23549–23557

Barzik M, Kotova TI, Higgs HN, Hazelwood L, Hanein D, Gertler FB, and Schafer DA (2005) Ena/VASP Proteins Enhance Actin Polymerization in the Presence of Barbed End Capping Proteins. J Biol Chem 280:28653–28662

Bear JE, Loureiro JJ, Libova I, Fässler R, Wehland J, Gertler FB (2000) Negative regulation of fibroblast motility by Ena/VASP proteins. Cell 101:717–28

Bear JE, Svitkina TM, Krause M, Schafer DA, Loureiro JJ, Strasser GA, Maly IV, Chaga OY, Cooper JA, Borisy GG, Gertler FB (2002) Antagonism between Ena/VASP proteins and actin filament capping regulates fibroblast motility. Cell 109:509–21

Bear JE, Gertler FB (2009) Ena/VASP: towards resolving a pointed controversy at the barbed end. J Cell Sci 122:1947–1953

Breitsprecher D, Kiesewetter AK, Linkner J, Urbanke C, Resch GP, Small JV, Faix J (2008) Clustering of VASP actively drives processive, WH2 domain-mediated actin filament elongation. EMBO J 27:2943–2954

Breitsprecher D, Kiesewetter AK, Linkner J, Vinzenz M, Stradal TEB, Small JV, Curth U, Dickinson RB, Faix J (2011) Molecular mechanism of Ena/VASP-mediated actin-filament elongation. EMBO J 30:456–467

Broedersz CP, Storm C, MacKintosh FC (2008) Nonlinear Elasticity of Composite Networks of Stiff Biopolymers with Flexible Linkers. Phys Rev Lett 101:118103

Chereau D, Dominguez R (2006) Understanding the role of the G-actin-binding domain of Ena/VASP in actin assembly. J Struct Biol 155:195–201

Ewoldt R H, Hosoi AE, McKinley GH (2008) New Measures for Characterizing Nonlinear Viscoelasticity in Large Amplitude Oscillatory Shear. J Rheo 52:1427-1458

Ferron F, Rebowski G, Lee SH, Dominguez R (2007) Structural basis for the recruitment of profilin-actin complexes during filament elongation by Ena/VASP. EMBO J 26:4597–4606

Furman C, Sieminski AL, Kwiatkowski AV, Rubinson DA, Vasile E, Bronson RT, Fässler R, Gertler FB (2007) Ena/VASP is required for endothelial barrier function *in vivo*. J Cell Biol 179:761–775

Galler AB, Garcia Arguinzonis MI, Baumgartner W, Smolenski A, Simm A, Reinhard M (2006) VASP-dependent regulation of actin cytoskeleton rigidity, cell adhesion, and detachment. Histochem Cell Biol 125:457–474

Gardel ML, Shin JH, MacKintosh FC, Mahadevan L, Matsudaira P, Weitz DA (2004) Elastic Behavior of Cross-Linked and Bundled Actin Networks. Science 304:1301–1305

Gardel ML, Nakamura F, Hartwig JH, Crocker JC, Stossel TP, Weitz DA (2006) Prestressed F-actin networks cross-linked by hinged filamins replicate mechanical properties of cells. Proc Natl Acad Sci USA 103:1762-1767

Hansen SD, Mullins RD (2010) VASP is a processive actin polymerase that requires monomeric actin for barbed end association. J Cell Biol 191:571–584

Hüttelmaier S, Harbeck B, Steffens NO, Meßerschmidt SI, Illenberger S, Jockusch BM (1999) Characterization of the actin binding properties of the vasodilator-stimulated phosphoprotein VASP. FEBS Letters 451:68–74

Kasza KE, Koenderink GH, Lin YC, Broedersz CP, Messner W, Nakamura F, Stossel TP, MacKintosh FC Weitz DA (2009) Nonlinear elasticity of stiff biopolymers connected by flexible linkers. Phys Rev E 79:041928

Koestler SA, Rottner K, Lai F, Block J, Vinzenz M, Small JV (2009) F- and G-actin concentrations in lamellipodia of moving cells. PLoS ONE 4:e4810

Krause M, Bear JE, Loureiro J, Gertler F B (2002) The Ena/VASP enigma. J Cell Sci 115:4721–4726

Kwiatkowski AV, Gertler FB, Loureiro JJ (2003) Function and regulation of Ena/VASP proteins. Trends Cell Biol 13:386–392

Kwiatkowski AV, Rubinson DA, Dent EW, van Ween EJ, Leslie JD, Zhang J, Mebane LM, Philippar U, Pinheiro EM, Burds AA, Bronson RT, Mori S, Fässler R, Gertler FB (2007) Ena/VASP Is Required for Neuritogenesis in the Developing Cortex. Neuron 56:441–455

Laurent V, Loisel TP, Harbeck B, Wehman A, Groebe L, Jockusch BM, Wehland J, Gertler FB, Carlier M-F (1999) Role of Proteins of the Ena/VASP Family in Actin-based Motility of Listeria monocytogenes. J Cell Biol 144;1245–1258

Lebrand C, Dent EW, Strasser GA, Lanier LM, Krause M, Svitkina TM, Borisy GG, Gertler FB (2004) Critical Role of Ena/VASP Proteins for Filopodia Formation in Neurons and in Function Downstream of Netrin-1. Neuron 42:37–49

Lieleg O, Claessens MMAE, Heussinger C, Frey E, Bausch AR (2007) Mechanics of Bundled Semiflexible Polymer Networks. Phys Rev Lett 99:088102–4

Lieleg O, Cyron CJ, Schmoller KM, Luan Y, Wall WA, Bausch AR (2009) Structural polymorphism in heterogeneous cytoskeletal networks. Soft Matter 5:1796–1803

Lieleg O, Claessens MMAE, Bausch AR (2010) Structure and dynamics of cross-linked actin networks. Soft Matter 6:218–225

Loisel TP, Boujemaa R, Pantaloni D, Carlier M-F (1999) Reconstitution of actin-based motility of Listeria and Shigella using pure proteins. Nature 401:613–616

Paluch E, van der Gucht J, Joanny J-F, Sykes C (2006) Deformations in Actin Comets from Rocketing Beads. Biophys J 91:3113–3122

Pardee JD, Spudich JA (1982) Mechanism of K+-induced actin assembly. J Cell Biol 93:648–654

Pasic L, Kotova TI, Schafer DA (2008) Ena/VASP Proteins Capture Actin Filament Barbed Ends. J Biol Chem 283:9814–9819

Plastino J, Olivier S, Sykes C (2004) Actin Filaments Align into Hollow Comets for Rapid VASP-Mediated Propulsion. Curr Biol 14:1766–1771

Pollard TD, Blanchoin L, Mullins RD (2000) Molecular mechanisms controlling actin filament dynamics in nonmuscle cells. Annu Rev Biophys Biomol Struct 29:545–576

Reinhard M, Jarchau, T, Walter, U (2001) Actin-based motility: stop and go with Ena/VASP proteins. Trends Biochem Sci 26:243–249

Samarin S, Romero S, Kocks C, Didry D, Pantalon, D, Carlier M-F (2003) How VASP enhances actin-based motility. J Cell Biol 163:131–142

Semmrich C, Larsen RJ, Bausch AR (2008) Nonlinear mechanics of entangled F-actin solutions. Soft Matter 4:1675-1680

Schirenbeck A, Arasada R, Bretschneider T, Stradal TEB, Schleicher, M, Faix J (2006) The bundling activity of vasodilator-stimulated phosphoprotein is required for filopodium formation. Proc Natl Acad Sci USA 103:7694–7699

Schmoller KM, Lieleg O, Bausch, A. (2009) Structural and Viscoelastic Properties of Actin/Filamin Networks: Cross-Linked versus Bundled Networks. Biophys J 97:83–89

Shin JH, Gardel ML, Mahadevan L, Matsudaira P, Weitz DA (2004) Relating microstructure to rheology of a bundled and cross-linked F-actin network in vitro. Proc Natl Acad Sci USA 101:9636–9641

Skoble J, Auerbuch V, Goley ED, Welch MD, and Portnoy DA (2001) Pivotal role of VASP in Arp2/3 complex–mediated actin nucleation, actin branch-formation, and *Listeria monocytogenes* motility. J Cell Biol 155:89–100

Suei S, Seyan R, Noguera P, Manzi J, Plastino J, Kreplak L (2011) The Mechanical Role of VASP in an Arp2/3-Complex-Based Motility Assay. J Mol Biol (in press)

Tempel M, Isenberg G, Sackmann E (1996) Temperature-induced sol-gel- transition and microgel formation in alpha-actinin cross-linked actin networks: A rheological study. Phys Rev E 54**:**1802–1808

Tobacman LS, Korn ED (1983) The kinetics of actin nucleation and polymerization. J Biol Chem 258:3207–3214

Trichet L, Campàs O, Sykes C, Plastino J (2007) VASP Governs Actin Dynamics by Modulating Filament Anchoring. Biophys J 92:1081–1089

Tseng Y, Wirtz D (2001) Mechanics and Multiple-Particle Tracking Microheterogeneity of α–Actinin-Cross-Linked Actin Filament Networks. Biophys J 81:1643-1656

Walders-Harbeck B, Khaitlina SY, Hinssen H, Jockusch BM, Illenberger S (2002) The vasodilator-stimulated phosphoprotein promotes actin polymerisation through direct binding to monomeric actin. FEBS Lett 529:275–280

Wiesner S, Helfer E, Didry D, Ducoret G, Lafuma F, Carlier M-F, Pantaloni D (2003) A biomimetic motility assay provides insight into the mechanism of actin-based motility. J Cell Biol 160:387–398

Xu J, Tseng Y, Wirtz D (2000) Strain Hardening of Actin Filament Networks. J Biol Chem 275:35866-35892

Yaba A, Kayisli U, Tanriover G, Demir N (2011) Spatial and temporal expression of vasodilator-stimulated phosphoprotein (VASP) in fetal and adult human cerebral cortex. Int J Dev Neurosci 29:131–136

Figure captions

Fig. 1 Schematic of VASP's domain structure and binding partners. **a.** Diagram of VASP's domains including EVH1, proline-rich and EVH2 domains. The EVH1 domain binds actin binding proteins such as zyxin, vinculin, and ActA. The proline-rich domain (Poly Pro) binds profilin, and the GAB and FAB domains bind monomeric and filamentous actin, respectively. TET is responsible for forming VASP tetramers. **b.** Diagram of VASP's tetrameric structure depicting actin filament binding via both GAB and FAB domains in the absence of free actin monomers. The EVH2 domain is known to be highly flexible and allows for multiple F-actin configurations when VASP is not confined to a substrate

Fig. 2 Effects of wild type VASP on F-actin network elasticity and morphology. The actin concentration is held fixed at c = 35.7 μM and the actin:VASP molar ratio is varied. **a (*Left*).** Frequency

dependence of the elastic modulus of VASP/actin networks for five VASP:actin molar ratios, *R* (Squares: actin-only; circles: *R* = 0.003; triangles up: *R* = 0.006); triangles down: *R* = 0.025; triangles left: *R* = 0.1). The weak dependence on frequency is characteristic of weakly viscoelastic solids. (*Right*) Dependence of the loss tangent, $tan\ \delta = G''/G'$, on *R*. The solid line indicates the reference value measured for a pure actin network. There is only a small decrease in the loss tangent with increasing VASP concentration, again consistent with weak crosslinking activity. **b** (*Lower*). Elastic plateau modulus, G_0, versus *R*, evaluated at an oscillation frequency of 1.15 rad/s. The value of G_0 for actin alone is shown as a horizontal line for reference. G_0 shows a maximum at an *R*-value of 0.006. (*Upper*) Confocal fluorescence images showing the microstructure of F-actin/VASP networks. Changes in overall network morphology as a function of *R* are consistent with the rheological behaviour. At *R* = 0.001, bundling is sparse, corresponding to a small increase in plateau modulus G_0. At *R* = 0.003, more bundles have formed and G_0 is increased. At *R* = 0.006, where G_0 is maximal, bundles are longer, thicker and more strongly curved and some small aggregates appear. At *R* = 0.0125, many bundles become incorporated into tangled aggregates and G_0 decreases. Finally, at *R* = 0.1 aggregates become very large and prominent and G_0 returns to near the value at low *R*. The scale bar applies to all images

Fig. 3 The nonlinear elastic response of VASP-mediated F-actin networks measured by LAOS. The ratio of the Chebychev coefficients e_3/e_1 provides a measure of the nonlinear network response. At *c* = 35.7 μM and *R* = 0.006, corresponding to the maximum increase in the linear elastic modulus, only a small degree of strain-stiffening due to the presence of VASP (squares) is observed. This strain-stiffening is not significantly different from that of F-actin alone (circles). (Inset) Lissajous curves showing stress $\sigma(t)$ as a function of applied strain $\gamma(t)$ for three strain amplitudes – 2.0% (innermost curve), 22.2% (middle curve), and 73.9% (outermost curve). The inner curve is elliptical indicating a linear response. Slight deviations from an ellipse are observed at higher strains (middle curve),

indicating intra-cycle stiffening. The outer curve shows significant distortion in the Lissajous curve as the network approaches mechanical failure and rupture.

Fig. 4 The effect of VASP's different actin binding domains on F-actin network elasticity and morphology evaluated by comparing wild type VASP (WT) with various mutants. **a.** Plateau moduli, G_0, evaluated at an oscillation frequency of 1.15 rad/s for F-actin polymerized in the presence of different VASP mutants at c = 35.7 μM and R = 0.025. All mutants cause crosslinking, as evidenced by an increase in network stiffness compared to pure F-actin (white bar). However, wild type VASP (black bar) produces a higher elasticity than any of the mutants (grey bars). Stiffening by the double mutant ΔFABGAB is not statistically significant compared to actin only. Complexing the GAB site of the ΔFAB mutant with latrunculin B-actin abolished crosslinking (hatched bar). Data with error bars are averages with standard deviations of 3 independent experiments. **b.** Confocal images of F-actin networks polymerized at c = 11.9 μM with wild type VASP or ΔFAB and ΔFABGAB mutants at R = 0.050. ΔFAB shows significant bundling, but less than wild type VASP, while ΔFABGAB shows only sparse bundles. The rightmost column shows the effect of addition of 4 μM latrunculin-actin to wild type, ΔFAB and ΔFABGAB samples. Latrunculin-actin eliminates bundling for the ΔFAB mutant, but has no effect for wild type or ΔFABGAB VASP. The scale bar applies to all images. **c.** Low speed sedimentation assay showing that all mutants bundle at R = 0.050 (significant amounts of actin present in the pellet, P), except for ΔFABGAB (nearly all actin present in the supernatant, S). **d.** Confocal fluorescence images comparing effects on F-actin network morphology between VASP wild type and the mutant VASPΔTET for c = 35.7 μM and R = 0.1. This mutant lacks the tetramerization site and demonstrates that VASP monomers produce significantly less bundling than full tetramers. The scale bar applies to all images

Fig. 5 The onset of VASP-mediated F-actin bundling depends upon actin concentration. The left-hand column shows homogeneous F-actin networks containing wild type VASP at the indicated actin:VASP molar ratio *R*. The middle column shows the first appearance of actin bundles at higher *R*. As the actin concentration is decreased, the bundling onset shifts to higher values of *R*. At all actin concentrations tested, large bundle aggregates were dominant at a molar ratio of $R = 0.05$ (right-hand column). The scale bar applies to all images

Supplementary Figure captions

Online Resource 1 Confocal fluorescence images showing F-actin networks in solutions containing Mg^{2+} concentrations of (a) 1.42 mM and (b) 5.18 mM. No significant difference in the degree or extent of bundling is apparent.

Online Resource 2 Homogeneous F-actin networks at three actin concentrations. **A.** 11.9 μM. **B.** 23.8 μM. **C.** 35.7 μM. The scale bar applies to all images

Online Resource 3 Confocal fluorescence images showing effects on F-actin network morphology by the mutant VASPΔFAB for $c = 11.9$, 23.8 and 35.7 μM. This mutant demonstrates that the GAB site alone is sufficient to produce F-actin bundles. The scale bar applies to all images

Online Resource 4 Confocal fluorescence images showing effects on F-actin network morphology by the double mutant VASPΔFABGAB for $c = 11.9$, 23.8 and 35.7 μM. Loose bundles are observed only at $c = 35.7$ μM and $R > 0.025$. The scale bar applies to all images

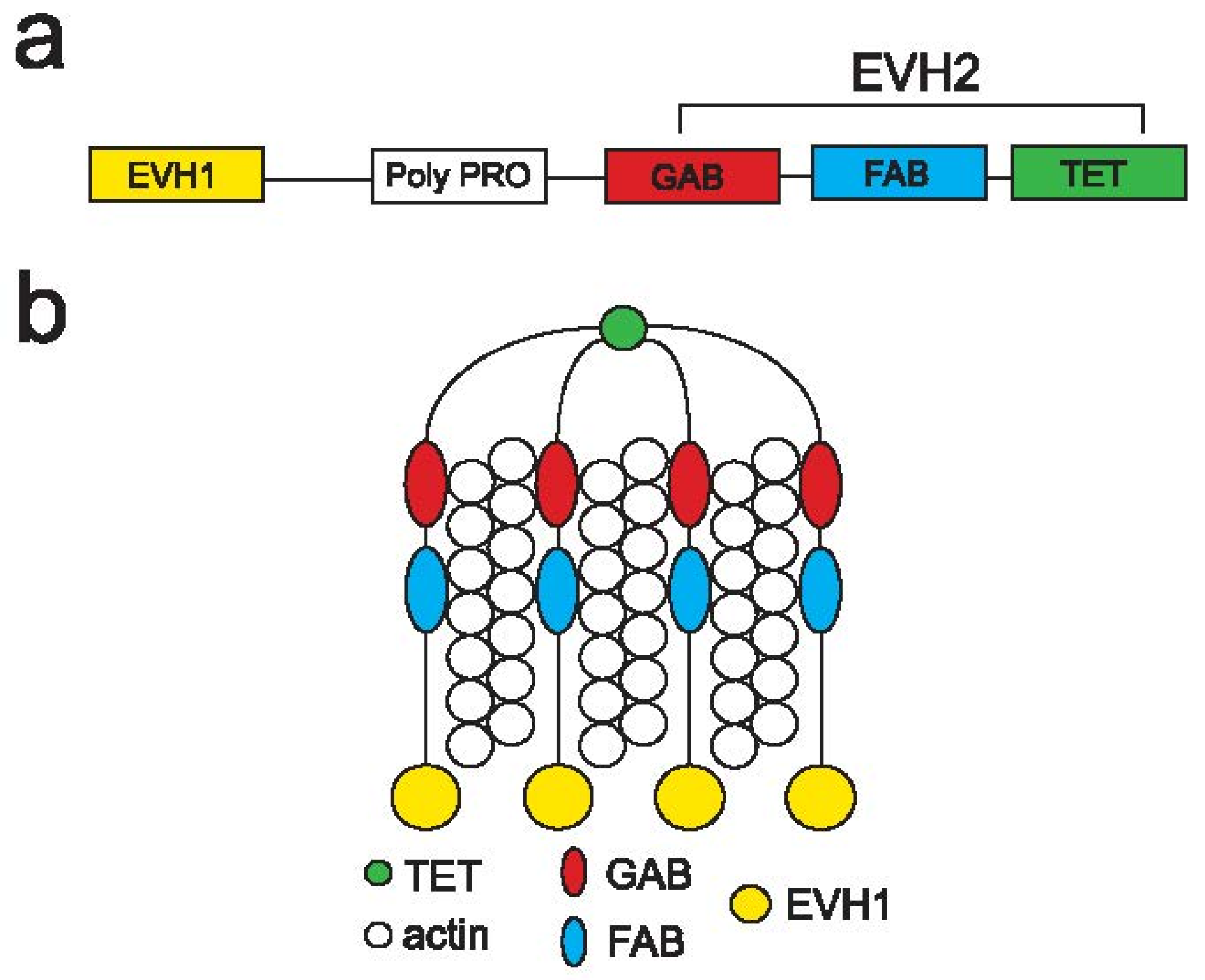
a
EVH2
EVH1
Poly PRO
GAB
FAB
TET
b
TET
GAB
EVH1
actin
FAB

Figure 2

A

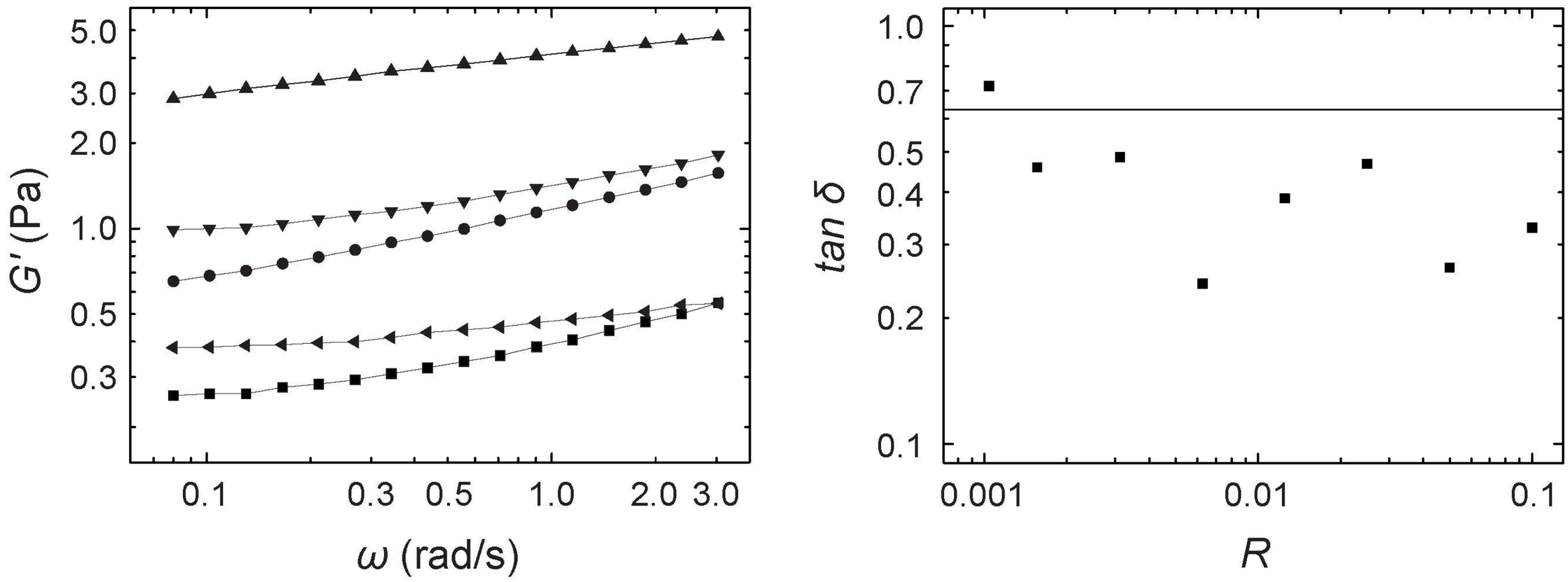
G' (Pa)
5.0
3.0
2.0
1.0
0.5
0.3
0.1
0.3
0.5
1.0
2.0
3.0
ω (rad/s)
tan δ
1.0
0.7
0.5
0.4
0.3
0.2
0.1
0.001
0.01
0.1
R

B

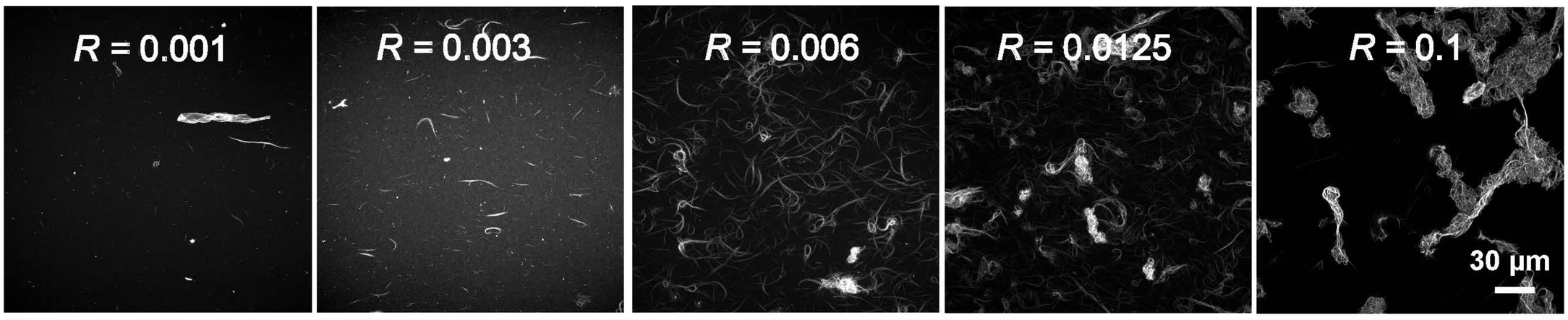
R = 0.001
R = 0.003
R = 0.006
R = 0.0125
R = 0.1
30 µm

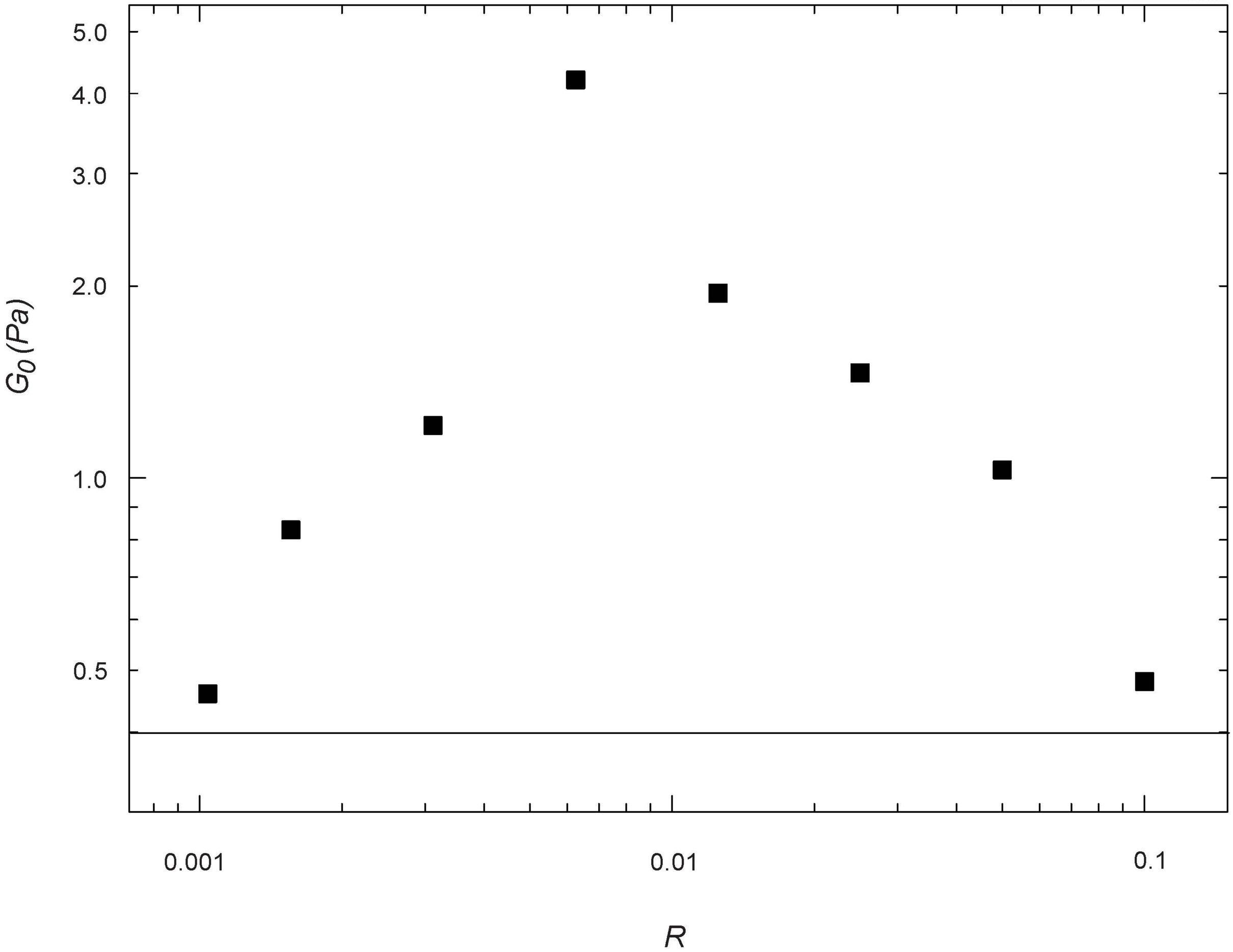
G0 (Pa)
5.0
4.0
3.0
2.0
1.0
0.5
0.001
0.01
0.1
R